ELECTROEXTRACTION ACROSS DROPLET-DROPLET INTERFACE

by

SUBHADEEP CHAKRABORTI

Presented to the Faculty of the Graduate School of

The University of Texas at Arlington in Partial Fulfilment

of the Requirements

for the Degree of

MASTER OF SCIENCE IN MECHANICAL ENGINEERING

THE UNIVERSITY OF TEXAS AT ARLINGTON

MAY 2019

Acknowledgements

I would like to dedicate this thesis to my parents. Their incessant motivation and sacrifices urged me to foray into the research field and prove my worth to the mankind as a human being.

I will always be grateful to Dr. Moon in my life for showing me the light of knowledge. She not only helps her students in being an independent researcher, but also prepares them for the rest of their lives.

I would like to extend my gratitude to Dr. Wen Shen and Dr. Miguel Amaya for being a part of my thesis defense committee.

A special thanks to Matin Torabinia and Shubhodeep Paul for their unconditional support during my research. Their constant mentoring and guidance helped me in gliding over the obstacles in my research. I thank Arvind Venkatesan for his mentoring in the initial stages of the research and helping me in the cleanroom fabrication.

May 10, 2019

Abstract

ELECTROEXTRACTION ACROSS DROPLET-DROPLET INTERFACE

Subhadeep Chakraborti, MS

The University of Texas at Arlington, 2019

Supervising Professor: Hyejin Moon

Extraction of analytes from solvents is a crucial part of many medical, clinical, industrial and refinery processes. It is required for preconcentration of analytes into other solvents, purification of solvents and detection of harmful or toxic molecules. One of the very important methods of extraction in microfluidics is liquid-liquid extraction (LLE). LLE involves the use of two immiscible liquids for diffusion of analytes across the interface. Recently there has been a growing interest in the coupling of external electric field with LLE to enhance the extraction of charged analytes. This has led to the birth of a new extraction method known as electroextraction. Although electroextraction has been mostly studied in continuous microfluidics, no significant effort has been made to integrate it with digital microfluidics for the development of lab-on-chip devices using electrowetting-on-dielectric (EWOD). As an initiation towards such integration, this thesis addresses the dependence of electroextraction across two stationary immiscible droplets on voltage, time and presence of surfactant. In this pursuit, an appropriate experimental set-up was designed with a coloured analyte. Then, a visual concentration measurement technique was developed using CIELAB color space and MATLAB code.

Table of Contents

List of Illustrations

List of Tables

Chapter 1

Introduction to liquid-liquid extraction

1.1 Liquid-liquid extraction (LLE)

In many industrial, chemical and biological laboratory processes, refineries etc. analytes of interest have to be separated from rest of the impurities present in the solution. Liquid-liquid extraction is a method to separate compounds based on their relative solubilities in two different immiscible liquids (usually water and organic solvent) having an interface. The difference in solubilities of the compounds arises from the differences in affinity of the compounds towards different liquids as shown in Figure 1.

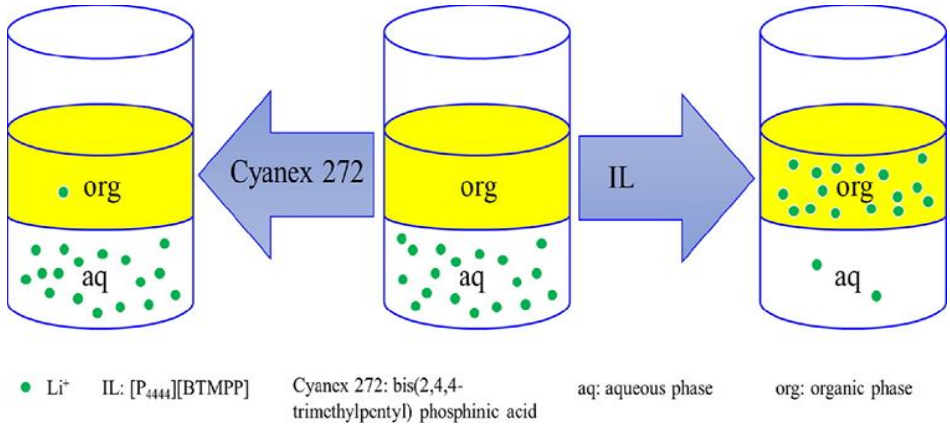

Figure 1 Partitioning of solutes in two immiscible liquids having an interface [1]

This distribution of solutes in two immiscible phases can be expressed by a dimensionless number called distribution coefficient (D) [2].

$$\log D_{octanol/water} = log\left(\frac{[solute]^{ionized}_{octanol}+[solute]^{unionized}_{octanol}}{[solute]^{ionized}_{water}+[solute]^{unionized}_{water}}\right)$$

where [solute] is the concentration of the solute. Analytes with negative log D are hydrophilic. Whereas, analytes with positive log D are hydrophobic.

In macroscale LLE (Figure 2), turbulence is created in the two phases to initiate mixing. In this process emulsion formation occurs. Although emulsion formation enhances extraction, separation of the two fluids is a difficult process. Use of large sample volumes, toxic organic solvents and time-consuming nature of this process are other demerits of LLE in macroscale. To circumvent the stated problems, LLE in microscale becomes pertinent.

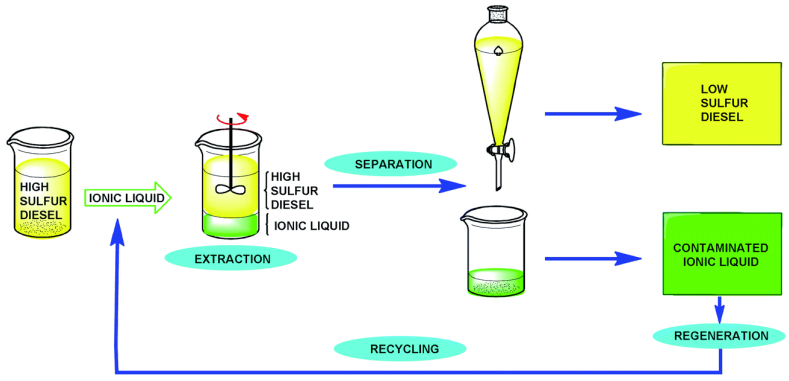

Figure 2 Extraction of sulfur from diesel [3]

1.2 LLE in microscale

LLE in microscale has been performed in both continuous and digital microfluidics. In 2012, Novak et al. extracted BSA (Bovine Serum Albumin) protein from D-fructose rich phase to ionic liquid (IL) in IL-Aqueous two phase system(ATPS) [4].

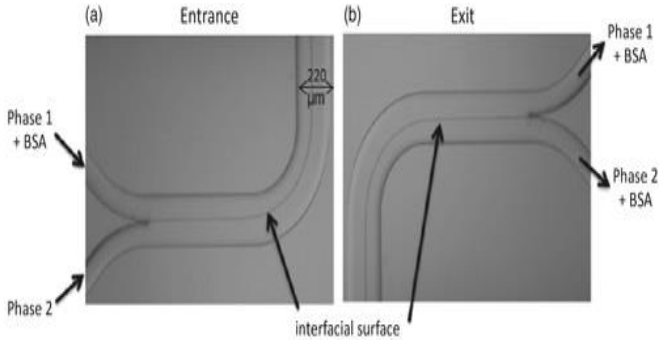

Figure 3 Extraction of protein in IL-ATPS [4]

As shown in Figure 4, Mary et al. demonstrated the extraction into and purification of droplets using fluorescent materials [5].

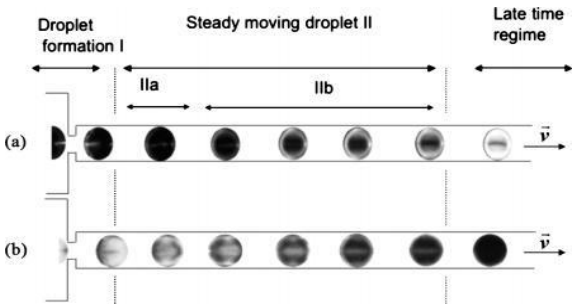

Figure 4 (a) Extraction of fluorescein from external phase to droplet (b) Purification: Extraction of rhodamine from droplet to external phase [5]

LLE in continuous microfluidics comes with some challenges such as separation of phases and dependence of extraction on flow of the phases. Improper phases separation or flow of phases would lead to undesired extraction results. To overcome these challenges digital microfluidics becomes a viable method because of its better control on discrete droplets as compared to that in continuous microfluidics. In 2011, Wijethunga et al. (Figure 5) extracted dye from aqueous solution to the ionic liquid (IL) on Electrowetting-on-dielectric (EWOD) platform [6].

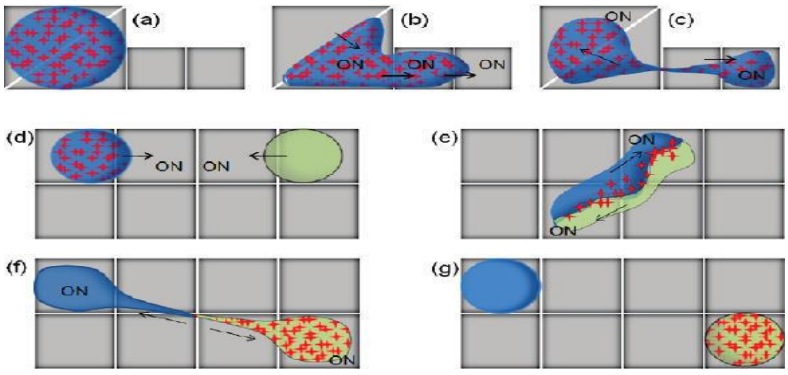

Figure 5 (a-c) Creation of donor (aqueous solution of dye) droplet, (d) Actuation of droplets to form interface, (e) Back and forth movement of droplets to enhance diffusion, (f-g) Separation of droplets [6]

Paul et al. extracted one of the constituent solutes into ionic liquid using EWOD [7]. Here the difference in the distribution coefficient of the solutes in the two solvents was utilized to achieve extraction (Figure 6). In addition to the steps shown in Figure 5, two cycles of extraction from the donor droplet was performed with fresh acceptor droplet taken before each cycle.

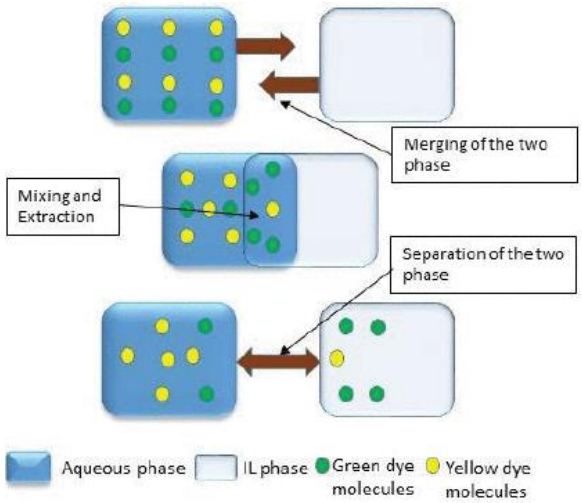

Figure 6 Selective extraction of green dye molecules from aqueous phase to IL phase [7]

Chapter 2

Literature review and research goals

2.1 Overview of electroextraction

LLE by itself is a passive extraction technique. It is dependent on the distribution coefficient of the analyte in two different phases. As a result, it relies on the natural diffusion of the analytes from one phase to another. So, LLE calls for the trial of different acceptor solvents in order to extract analytes from a particular donor solution. This process in some cases might not be economical. However, instead of trying out different acceptor solvents, the natural diffusion can be altered by using some kind of external field helping the analytes to cross the Gibb's free energy barrier at the interface. Electroextraction is one such active extraction process which alters the diffusion of charged analytes using electric field. In 1993, Benjamin et al. performed the molecular dynamics simulation of chloride ion transfer across water-dichloroethane interface [8]. This study considered the interface to be a diffused one. The free energy of transfer from water to the DCE phase found by simulation was close to that obtained experimentally.

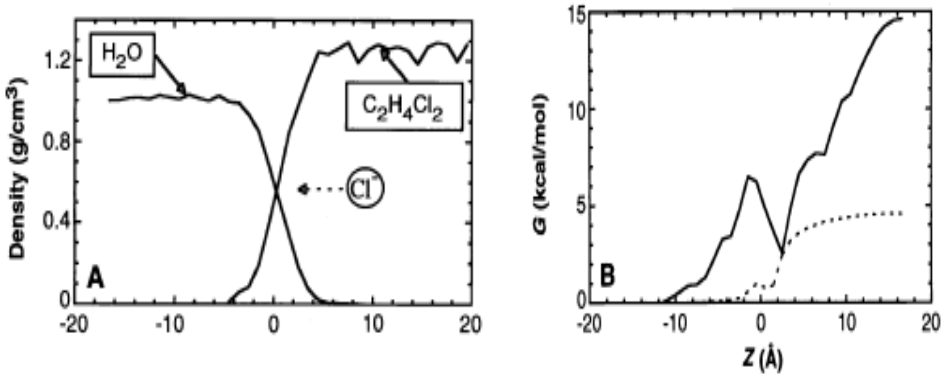

Figure 7 (A) Density profile across water-DCE interface (B) Gibb's free energy profile across the interface [8]

Electroextraction has been used for preconcentration and isolation of charged analytes. One of the applications of electroextraction is the extraction of charged drug molecules from aqueous-based samples like human urine and plasma to aqueous acceptor solution [9]. An organic solvent inside a physical membrane was used to separate the two miscible aqueous-based sample and acceptor solutions. Sample clean-up from biological fluids was achieved so as to isolate the drug molecules from the biological matrix and get improved detection of drugs present in the biological fluids.

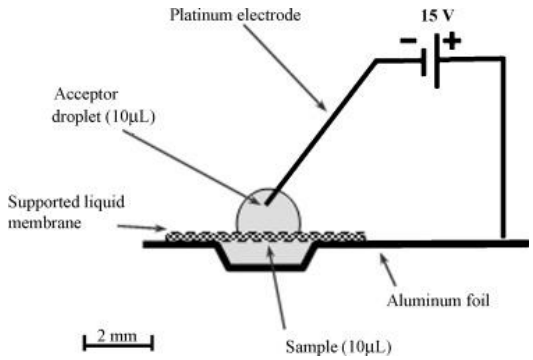

Figure 8 EME of positively charged drug molecules [9]

Electroextraction has also been used for size separation of DNA samples across the interface of ATPS [10]. In this case, the charge of the DNA was a differentiating factor as the charge is directly proportional to the size of the DNA molecule. Similarly, amino acids have been separated using electroextraction based on their different electrophoretic mobility (Figure 10) [11].

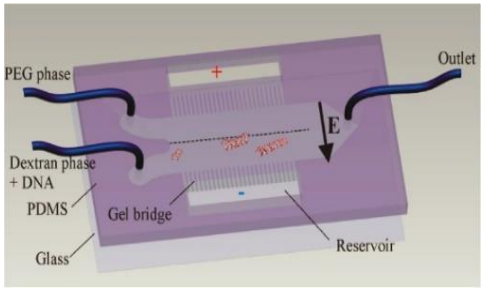

Figure 9 Size separation of DNA [10]

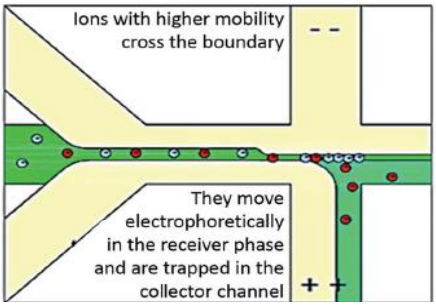

Figure 10 Separation of amino acids [11]

2.2 Objectives of research

All aforementioned applications of electroextraction suffer from some limitations. The first one is the separation of phases after extraction. It is a difficult process due to less control over the individual phases. The second limitation is the dependence of electroextraction on the flow of the phases. Improper separation would lead to getting undesired results. These limitations can be overcome by coupling of electroextraction with digital microfluidics i.e. EWOD. The possible sequence of performing electroextraction using droplets of two immiscible phases is shown in the Figure 11.

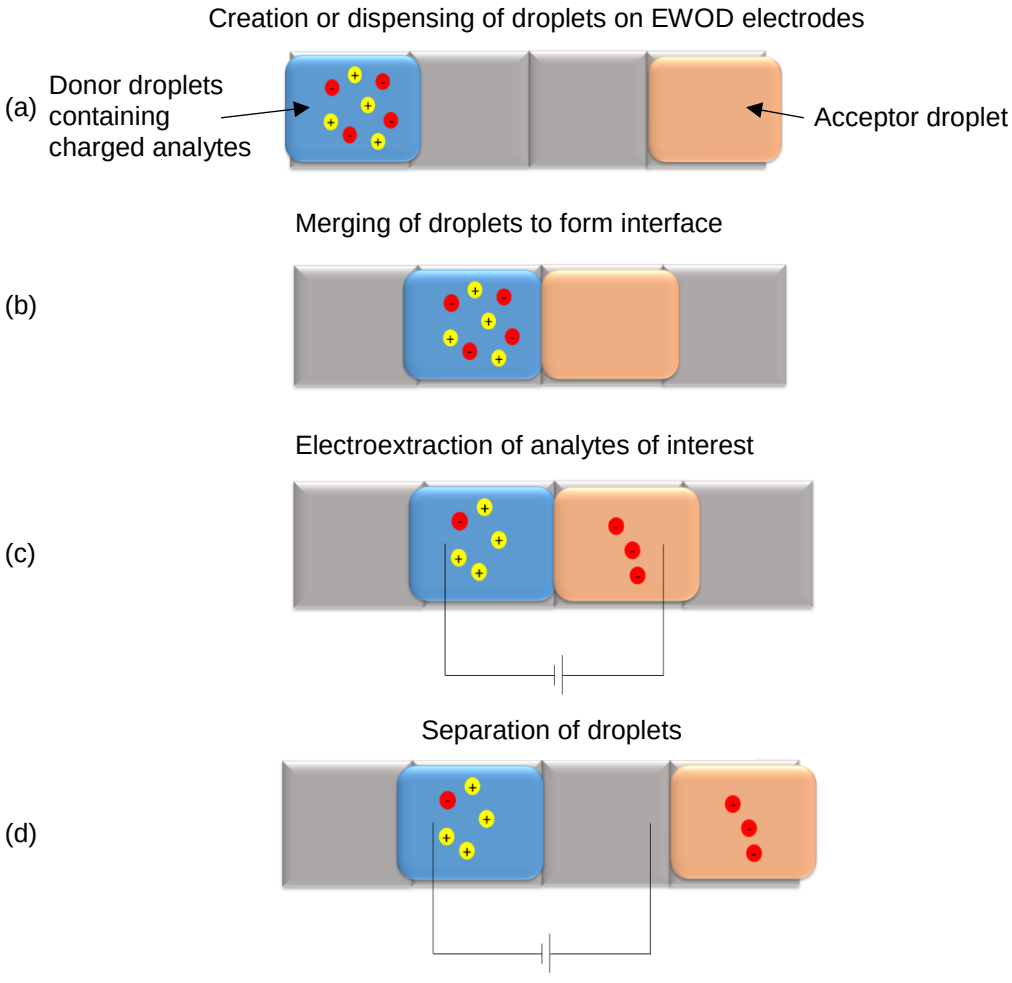

Figure 11 Electroextraction on EWOD platform (a-d)

The first step in this process is the creation of or dispensing donor droplet (containing charged analytes) and acceptor droplets. Then, the two droplets are merged to form an interface. A DC voltage is applied across the interface to selectively extract analytes of interest. Lastly, the droplets are separated for further postprocessing of the extracted analytes. But, before a device is designed to perform the above-mentioned tasks, the dependence of electroextraction on voltage, time, interfacial tension needs to be done.

The objectives of this research are as follows:

1. To characterize the dependence of electroextraction on voltage (time being constant),
2. To characterize the dependence of electroextraction on time (voltage being constant),
3. Qualitative study of the effect of surfactant on electroextraction.

Chapter 3

Materials and methods

3.1 Overview of experimental set-up

Initially the experimental set-up was designed as simple as possible so as to figure out the correct materials and experimental set-up design for this research by running qualitative tests. The basic requirements for the experimental set-up are charged analytes, donor solvent and acceptor solvent. It was preferable to have a coloured analyte so as to visually see the occurrence of electroextraction. The blue-coloured dye Acid Blue 80 was found to be an ionic compound as shown in Figure 12 [12].

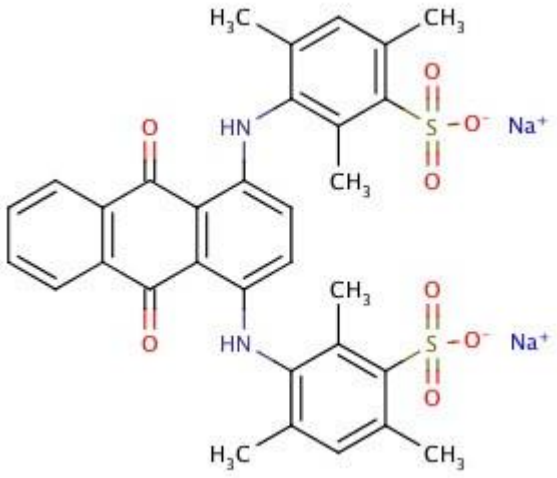

Figure 12 Chemical structure of Acid Blue 80 [12]

Based on the properties of most coloured organic compounds [13], it was inferred that the dye molecules dissociate in water into positive sodium ions and negative hydrocarbon ions. The colour of the dye is due to the excitation of electrons in the negative hydrocarbon group. The excitation of electrons is made easier by the aromatic rings.

Based on the above inferences, water was taken as the donor solvent. Ionic liquid (IL) 1-butyl-3- methylimidazolium hexafluorophosphate ([bmim][PF6]) was taken as the acceptor solvent . ILs have been previously used for extraction of analytes from aqueous solution [14], [15]. As shown in Figure 13, the positive electrode will be in the acceptor droplet, while the negative electrode will be in the donor droplet. This is done so as to cause electrophoretic motion of negatively charged hydrocarbon group towards the positive electrode. Bare silver-plated copper 30 gauge (0.15 mm) wires were used as electrodes. The electroextraction of the negatively charged hydrocarbon group will be characterized by the increase in the intensity of blue colour in the acceptor droplet.

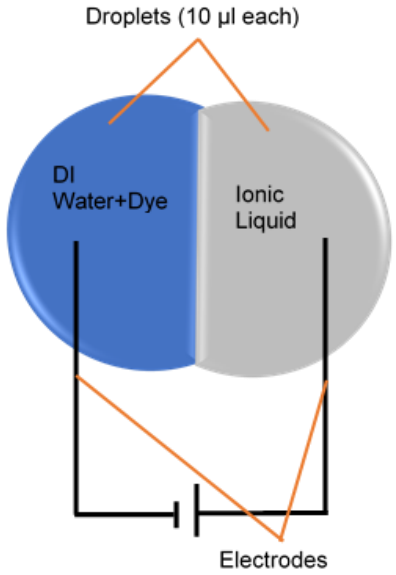

Figure 13 Schematic diagram of experimental set-up

The electrodes were connected to a DC power source. Visualization tests were conducted with (2 V) and without (0 V) voltage. The aim of these visualization tests was to see the proof of concept of electroextraction with the current experimental set-up. The results are shown in Figure 14. Experiments were conducted with voltages beyond 2 V to visually see the dependence of electroextraction on voltage.

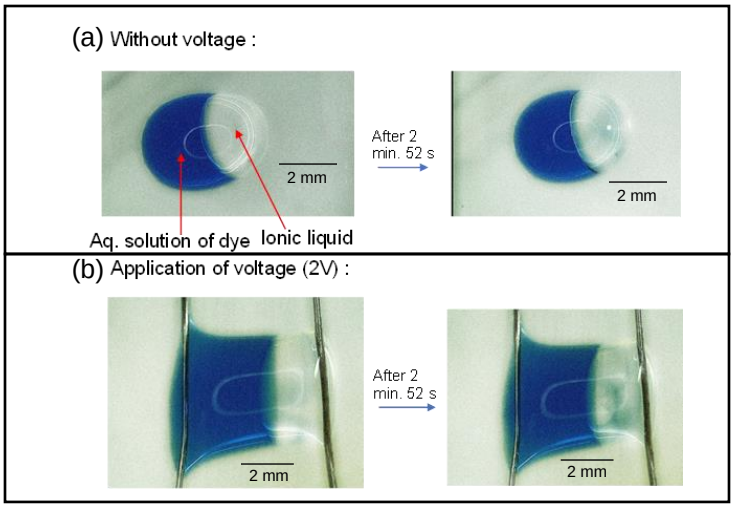

Figure 14 Comparison of results of normal diffusion (a) and electroextraction (b)

In Figure 14, the accumulation of dye analytes can be seen in the acceptor solvent near the electrodes. Although this qualitative test shows the proof of concept, there are some challenges that were faced during the experiments. The first one is that the electroextraction in IL is limited by its high viscosity (109 cP). Secondly, beyond 3V electrolysis was seen. Thirdly, the interface length is not constant in the results shown above. Thus, making this experimental set-up unfit for doing parametric studies stated in section 2.2. The first two challenges can be overcome by choosing a solvent of low viscosity so as to see a more vigorous electroextraction. 1-Octanol has been reported as supported liquid membrane solvent for electromembrane extractions [16]. Also, the viscosity of 1-Octanol (7.36 cP) was much lesser than that of IL. Visualization tests with and without voltages were run with 1-Octanol as the acceptor solvent (Figure 15).

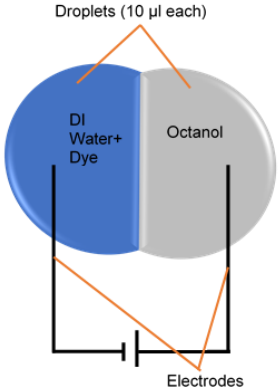

Figure 15 Experimental set-up using 1-Octanol as acceptor solvent

Figure 16 shows the results of the visualization tests using 1-Octanol as the acceptor solvent.

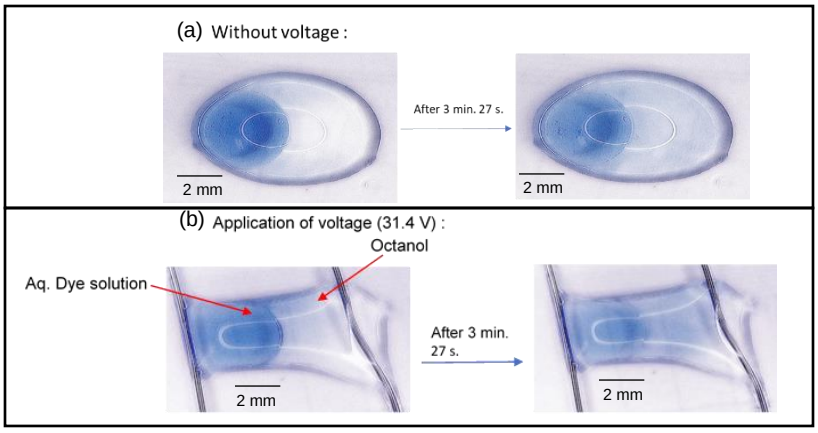

Figure 16 Visualization test results (a and b) using 1-Octanol as acceptor

In Figure 16, the accumulation of dye analytes in the acceptor solvent can be seen. Also, the electroextraction is more vigorous than in the IL case due to the lesser viscosity. No electrolysis was seen even at 31.4 V. The octanol was chosen as the acceptor solvent for rest of the experiments.

In order to have a constant interface length, the sandwiched configuration of the above experimental set-up was thought of a possible solution. As shown in Figure 17, it was needed to have planar electrodes.

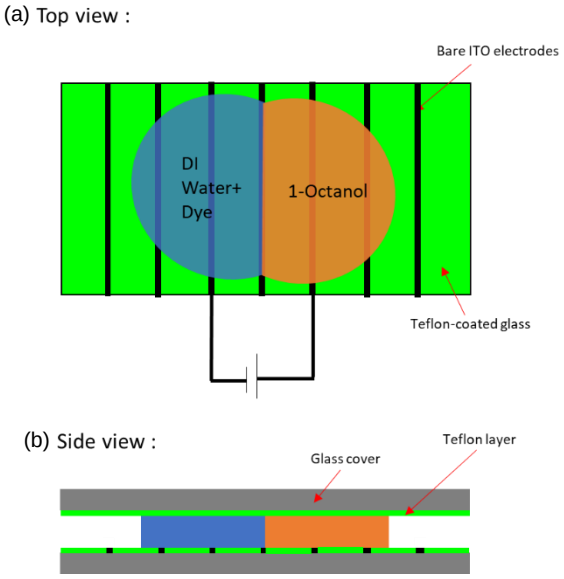

Figure 17 Schematic illustration of sandwiched configuration

The bottom chip having the planar electrodes was fabricated using cleanroom MEMS fabrication process as shown in Figure 18.

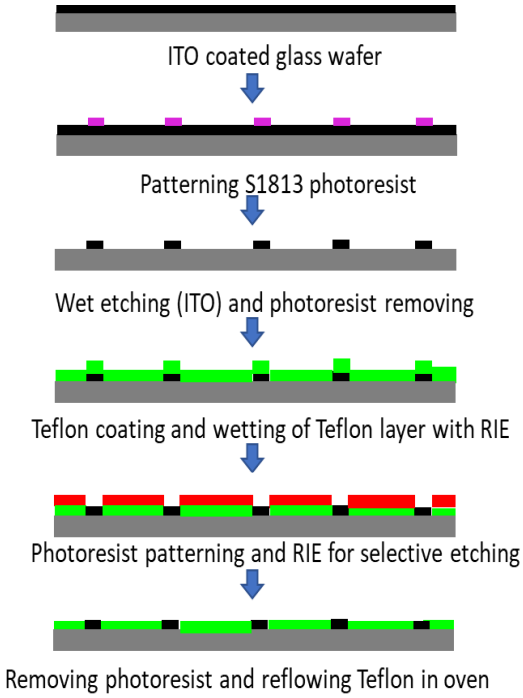

Figure 18 Bottom chip fabrication steps

The bottom chip and glass cover were coated with Teflon so as to have a hydrophobic surface which would prevent the excessive spreading of the droplets. The area of the bare ITO electrodes was very less as compared to rest of the area. As a result, spreading of the droplets on the electrodes was negligible on the electrodes. A gap of 80 microns was maintained between the bottom chip and the Teflon-coated glass cover using spacer tapes. However, repeatable identical interface between the droplets could not be attained using this experimental set-up. A different irregular interface was generated every time as shown in Figure 19. This was due to the fact that 1-Octanol has lower surface tension than that of water [17]. As a result, the spreading of 1-Octanol is higher than that of water during the sandwiching of droplets. Since the process of creating this sandwiched configuration was completely manual, slightest errors in sandwiching would lead to

unidentical interfaces every time.

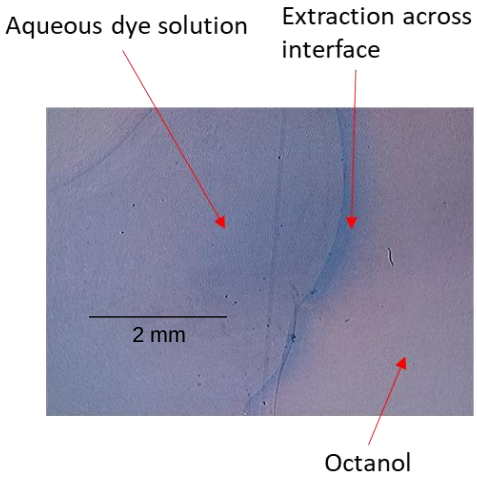

Figure 19 Sandwiched configuration interface

A possible solution to control the spreading of 1-Octanol is to have two intersecting circular compartments so as to contain the two liquids and have a repeatable identical interface. This idea was executed by having a PDMS (Polydimethylsiloxane) well as shown in Figure 20.

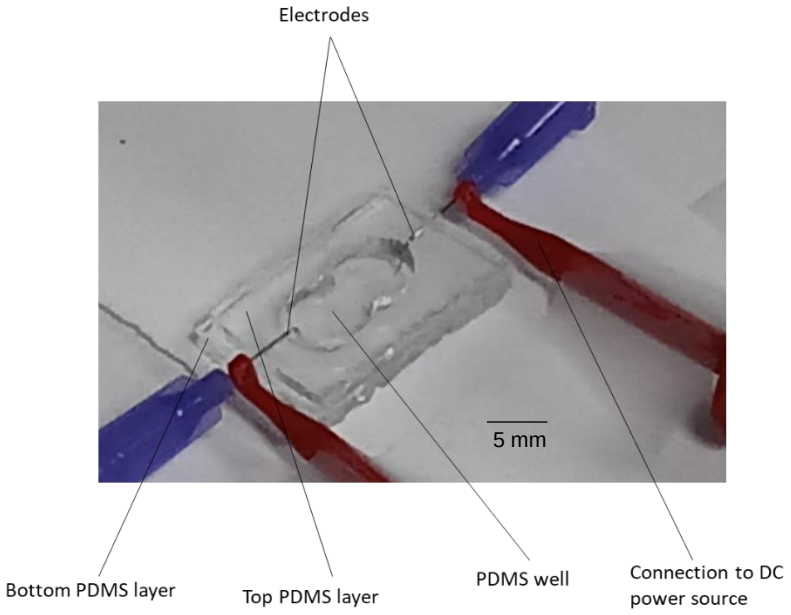

Figure 20 PDMS-well device

PDMS well consisted of two layers of PDMS each of thickness 2 mm. The top layer was punched to have two intersecting circular holes of diameters 0.8 cm as shown in Figure 20. The intersection points were 0.5 cm apart. To close the holes from one side, another PDMS layer was bonded to the top layer using super glue. Consequently, two intersecting circular well compartments were formed. 30 Ga. Stainless steel industrial dispensing tips were bent near the dispensing tips at right angles to form electrodes of length same as the depth of the well. The electrodes were 1.1 cm apart. White A4 sheet paper was used as background. Identical interface could be obtained every time the two phases were dispensed in the PDMS well as shown in Figure 21.

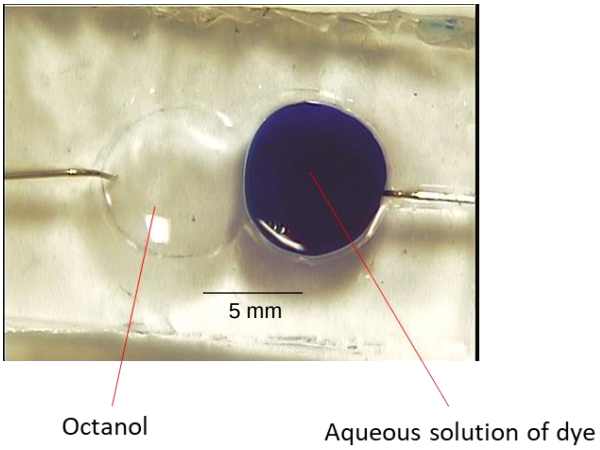

Figure 21 Snapshot of interface in PDMS-well device

Three qualitative tests were performed with the above experimental set-up. The details of the tests are specified in Table 1.

Table 1 Qualitative tests

Voltage	Positive terminal in	Negative terminal in
145.5 V	Acceptor droplet	Donor droplet
0 V	-	-
145.5 V	Donor droplet	Acceptor droplet

Images of the experiments were recorded at 10 minutes interval till 20 minutes. The results of the experiments are shown in Figure 22.

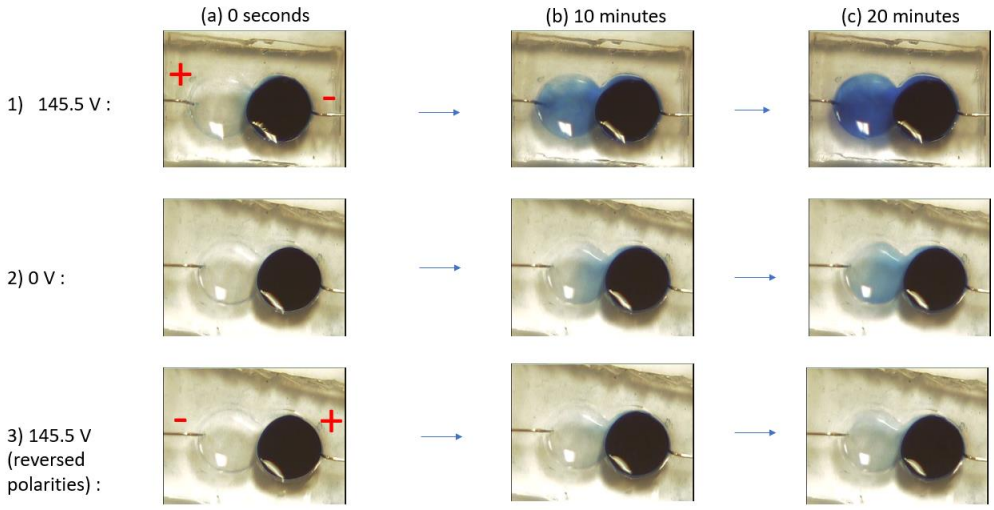

Figure 22 Snapshots of qualitative study experiments

The first two cases shown in Figure 22 shows the proof of concept of electroextraction. At 0 V normal diffusion of the dye occurs across the interface. When the positive electrode is present in the 1-Octanol phase, the electrophoretic force on the negatively charged analytes causes them to cross the Gibb's free energy barrier at the interface, thus increasing the extraction. This can be seen by the higher intensity of blue colour in the first case (in Figure 22) as compared to the 0 V case. However, when the polarities are reversed keeping the voltage same (145.5 V), the extraction is lower than that at 0 V as can be seen in the third case in Figure 22. This is possibly due to the increase in the Gibb's free energy across the interface resulting from electrophoretic force resisting the diffusion. In addition to enhancing extraction, electroextraction can reduce extraction. This is useful in cases where the extraction of certain analytes is not wanted.

Now that in the qualitative tests, it was visually established that electric field can enhance as well as impede extraction of charged analytes across the interface of two immiscible phases, the parametric studies stated in section 2.2 can be done.

3.2 Experimental procedure

The experimental set-up for conducting parametric studies is shown in Figure 23.

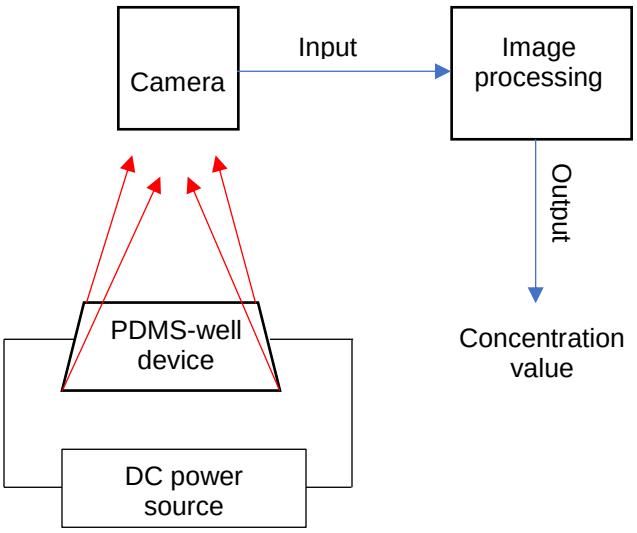

Figure 23 Experimental set-up for parametric studies

As stated in section 2.2, the objective of this research was to characterize dependence of electroextraction on voltage and time. Also, the effect of surfactant on electroextraction had to be qualitatively studied. The electric field in PDMS-well device was provided by Agilent Technologies N5750A System DC Power Supply. The electroextraction of analytes was measured in terms of decrease in the concentration of negatively-charged dye analyte in aqueous solution. The concentration was measured visually as change in the concentration of analytes results in the loss of intensity of the colour. In other words, high concentration of the analytes will result in dark blue colour. Whereas, low concentration of the analytes will result in pale blue colour. The videos of the experiments were captured using Hitachi CCD Color Camera (Model: KP-D20BU) attached to Fujinon-TV Zoom Lens. The camera was connected to the computer through Dazzle DVC 100 video capture card device.

3.3 Concentration measurement

As explained in section 3.2, the intensity of blue colour depends on the concentration of the negatively charged dye analytes. Consequently, there was a need to come up with a visual concentration measurement technique.

Any image is composed of several pixels. The colour of every pixel is a combination of certain proportions of red, green and blue colours. In RGB (Red Green Blue) system, a pixel has certain values of red (r), green (g) and blue (b) according to their proportions. However, with the variation in brightness of an image, the r, g and b values change. The RGB system is not able to indicate the true colour of an object in the presence of varying illumination. Thus, if RGB system is used for recording concentration change, change in r, g and b values does not necessarily mean that there is a change in concentration. Rather, the change in the values might be due to the change in surrounding illumination. CIELAB color space is one of the various colour spaces available that differentiate between the true colour of an image and illumination. The schematic representation of CIELAB color space is shown in Figure 24.

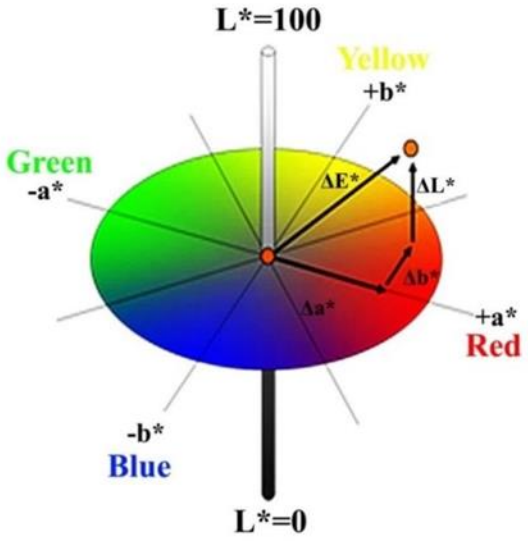

Figure 24 CIELAB color space [18]

The true colour is given by a and b values. The a value ranges from -a^* to a^*. The b value ranges from -b^* to b^*. The illumination is specified by a separate parameter known as L^*.

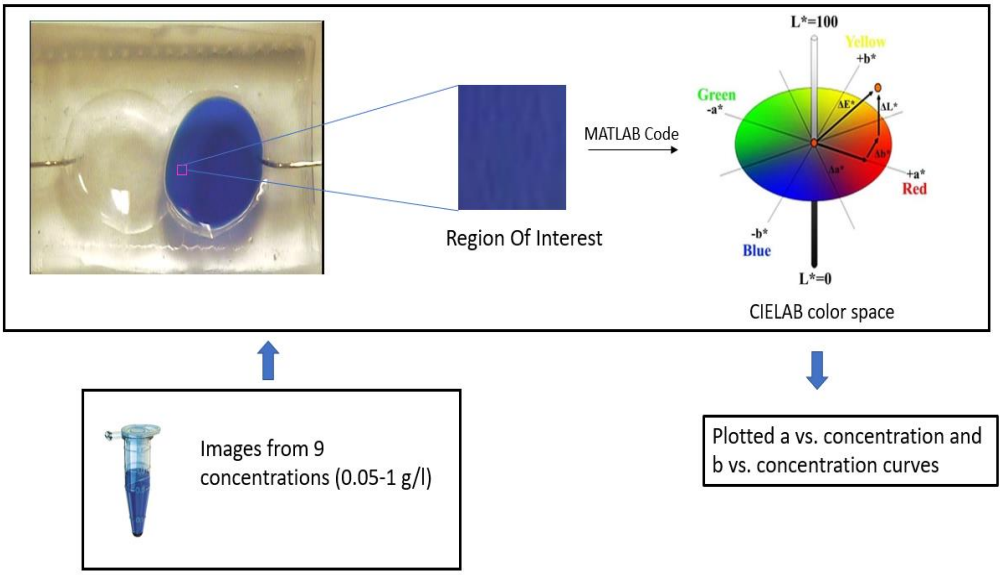

Figure 25 a and b values vs. concentration calibration procedure

As shown in Figure 25, the calibration of a and b values vs. concentration was performed. A region of linear dependence of a and b values on concentration was sought. The calibration procedure is as follows:

1. Nine concentrations ranging from 0.05 g/l to 1 g/l were prepared.
2. The solutions as well as 1-Octanol were dispensed in the PDMS-well device. Images were captured using the experimental set-up explained in section 3.2. Both the phases were dispensed to prevent any dissimilarity with parametric study images.
3. Average a and b values of a region of interest (containing group of pixels) in the aqueous phase were computed using a MATLAB code (present in Appendix) prepared during this research. Instead of 1-Octanol, aqueous phase was chosen for

this purpose because the dye homogenizes faster in the aqueous phase than in the 1-Octanol phase.

4. Average a and b values were plotted against concentration. Consequently, calibration curves of a vs. concentration and b vs. concentration were generated.
5. After inspecting both the curves, linear region with R-squared value of 0.9892 was obtained in b vs. concentration curve in the concentration range of 0.05-0.15 g/l as shown in Figure 26.

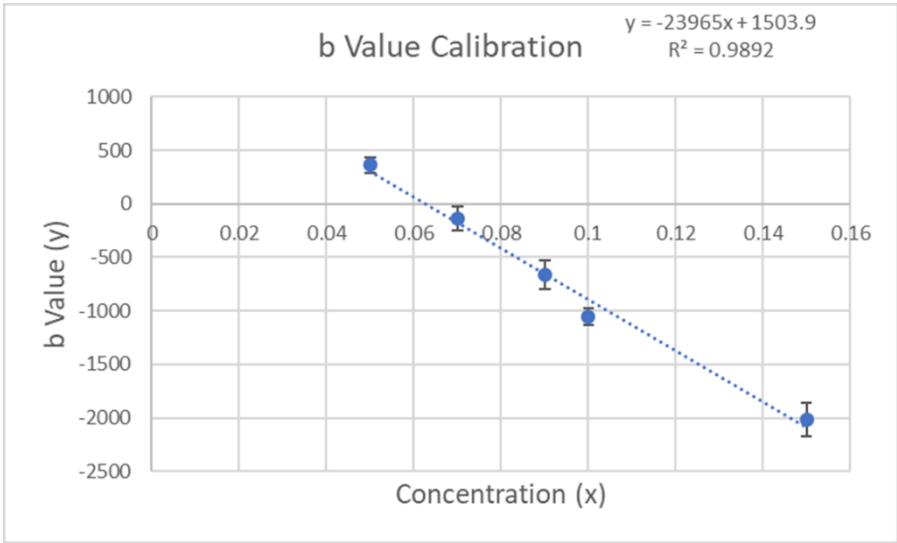

Figure 26 Linear segment of b vs. concentration calibration curve

As can be seen from Figure 26, the initial concentration for the parametric studies was chosen as 0.15 g/l. The highest concentration in the linear range was considered so as to have the final concentrations after electroextraction within the linear range.

Chapter 4

Results and analysis

4.1 Electroextraction vs. voltage dependence

The dependence of electroextraction on voltage was measured by recording the change in concentration of aqueous solution. 70 microlitres of 0.15 g/l aqueous solution and 1-Octanol are dispensed in the PDMS-well device. The concentration change was recorded for 10 minutes at 0 V, 20.8 V, 40.6 V, 60.3 V, 80 V and 100.8 V. All the experiments were repeated four times. For each experiment, b values (average b value in a region of interest) were computed using the procedure outlined in section 3.3. For each b value, concentration was calculated using the equation of the calibration curve in Figure 26. Mean and standard deviation values of the concentrations were calculated at all the voltages. Then, they were plotted along with corresponding voltages as shown in Figure 27.

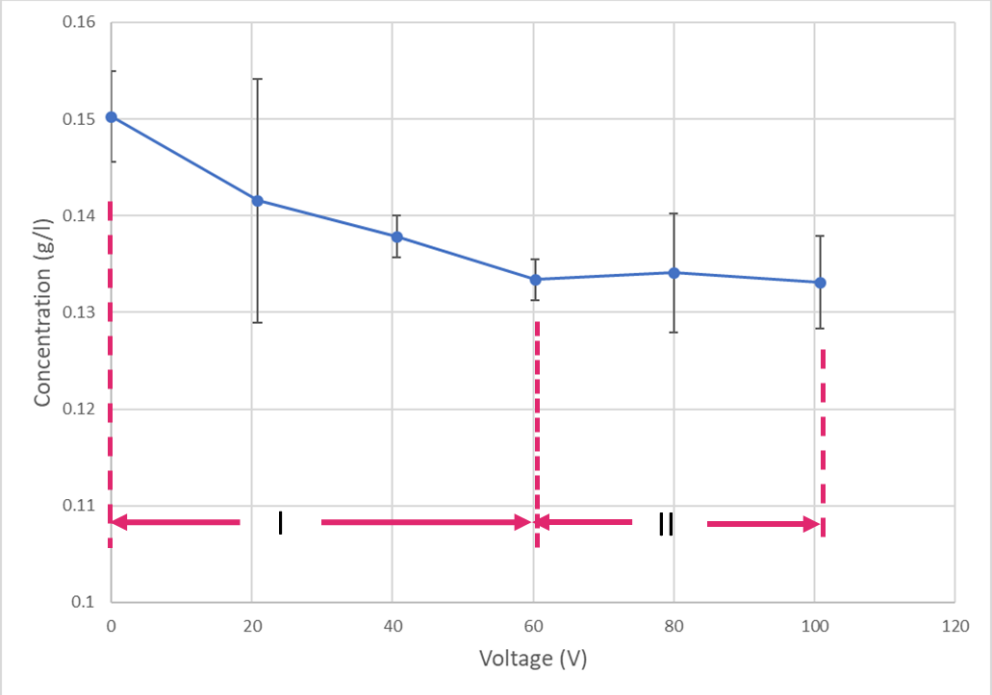

Figure 27 Concentration-voltage curve

The graph shown in figure consists of two regions which are as follows:

1) Region I: This region indicates the decrease in concentration of the aqueous solution of dye. As the voltage is increased, the Gibb's free energy barrier at interface is decreased. Hence, the number of negatively-charged analytes crossing this barrier is increasing. In other words, the electrophoretic force on the analytes is helping them to cross the Gibb's free energy barrier at the interface.
2) Region II: This region indicates the saturation of extraction in the 1-Octanol. Consequently, the curve becomes flat in this region. Although the electric field is increasing, the concentration is not changing.

It can be inferred from this study that for a particular duration of time, the electroextraction becomes limited at a certain voltage. Thus, it is wrong to expect that the concentration of the donor solution (aqueous solution of dye in this research) will keep on decreasing with voltage increasing indefinitely. All the analytes cannot be extracted across the interface by applying electric field for a particular duration of time.

4.2 Electroextraction vs. time dependence

The dependence of electroextraction on voltage was measured by recording the change in concentration of aqueous solution. 70 microlitres of 0.15 g/l aqueous solution and 1-Octanol are dispensed in the PDMS-well device. The concentration change was recorded for 4, 8, 12, 16 and 20 minutes at 100.8 V. All the experiments were repeated four times. For each experiment, b values (average b value in a region of interest) were computed using the procedure outlined in section 3.3. For each b value, concentration was calculated using the equation of the calibration curve in Figure 26. Mean and standard deviation values of the concentrations were calculated for all the time durations

mentioned above. Then, they were plotted along with corresponding time durations as shown in Figure 28.

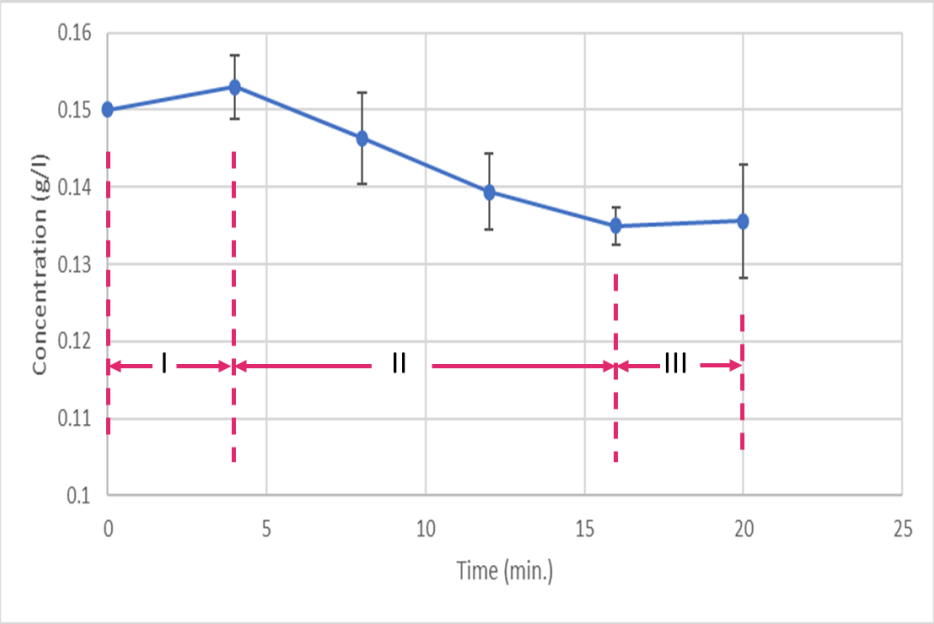

Figure 28 Concentration vs. time curve

The curve shown in Figure 28 consists of three regions which are as follows:

1) Region I: In the region I, there exists an anomaly such that the concentration increases. The concentration measured was of a small region near the interface. Initially, aggregation of the dye analytes occurs near the interface. As a result, an increase in the concentration is recorded initially.
2) Region II: In region II, the concentration of the aqueous solution of negatively-charged dye analytes decreases. Gradually the aggregated analytes start crossing the interface to reach the other phase (1-Octanol). The electrophoretic force on the analytes helped them to cross the Gibb's free energy barrier at the interface.
3) Region III: In region III, the curve is almost flat. This indicates there is a saturation of analytes in 1-Octanol. With the passage of time in this region, there is no net

extraction of analytes into 1-Octanol.

The inference from this study is that at a particular voltage, the extraction does not occur indefinitely. There is a limit to electroextraction at a certain point of time for a particular electric field.

4.3 Effect of surfactant on electroextraction

Surfactants are known to reduce the surface tension at the interface of two phases. This can possibly enhance liquid-liquid extraction. The aim of this study was to qualitatively see the effect of surfactant coupled with electroextraction. Three cases were considered for this study as detailed in Table 2. 0.7% aq. solution of surfactant Tween 20 was used along with dye analytes present in the same aqueous solution.

Table 2 Qualitative tests involving surfactant

Voltage	Positive terminal in	Negative terminal in
145.5 V (with surfactant)	Acceptor droplet	Donor droplet
145.5 V (without surfactant)	Acceptor droplet	Donor droplet
0 V (with surfactant)	-	-

Images of the experiments were recorded at 10 minutes interval till 20 minutes. The results of the experiments are shown in Figure 29.

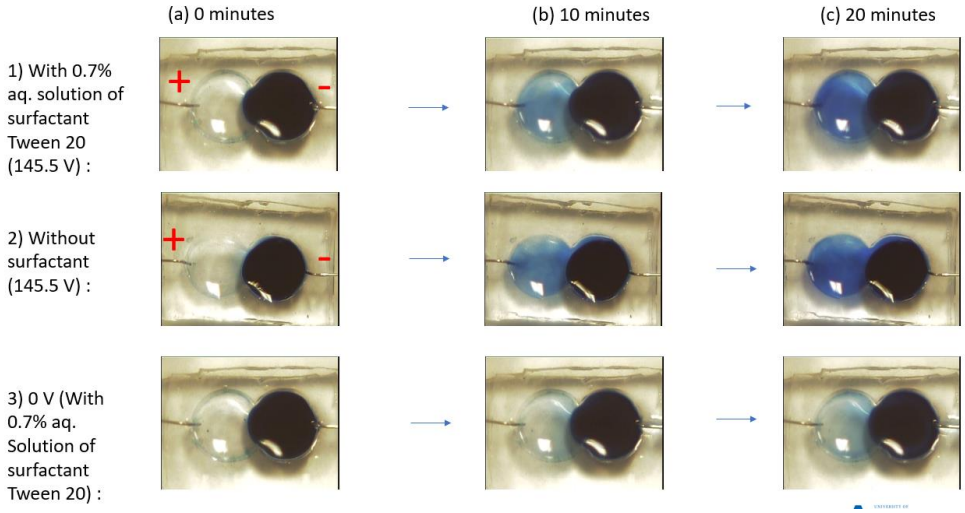

Figure 29 Snapshots of experiments involving surfactant

No significant difference between with and without surfactant cases (both having 145.5 V) can be seen in Figure 29. Clearly, there is increase in the extraction when electric field is applied in the presence of surfactant. However, the surfactant does not seem to further increase the extraction. One possible reason can be that 1-Octanol is itself an amphiphilic compound.

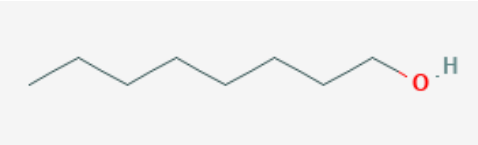

Figure 30 Chemical structure of 1-Octanol [19]

As can be seen in Figure 30, 1-Octanol has a hydrophilic part (O-H) and lipophilic hydrocarbon. Consequently, 1-Octanol itself is able to reduce the surface tension at the interface with water. Therefore, addition of a surfactant might not change the scenario significantly. However, it can be noted in Figure 29 that the interface length, upon addition of surfactant, is different from what it is in without surfactant case. Thus, the

design of the device has to be changed to have constant interface for fair comparison. Also, in addition to qualitative studies, parametric studies as done without surfactant in this research needs to be done with surfactant to quantitatively study the effect of surfactant on electroextraction.

Chapter 5

Conclusions and future work

The following conclusions were established by this research:

1) Qualitative study of electroextraction was performed. The proof of concept of electroextraction was shown. Various experimental set-ups were tested for this purpose. A PDMS-well device was made and utilized for the purpose of having constant interface so as to do qualitative as well as quantitative studies.
2) An image-based concentration measurement method was developed to do parametric study i.e. dependence of electroextraction on voltage (time being constant) and dependence of electroextraction on time (voltage being constant). A MATLAB code, prepared during this research, used CIELAB color space for concentration measurement purpose.
3) The dependence of electroextraction on electric field for a fixed duration of time was quantitatively analysed using concentration vs. voltage curve.
4) The relation between electroextraction and time of voltage applied was demonstrated using concentration vs. time curve.
5) The effect of viscosity on electroextraction was qualitatively demonstrated using two different extractants.
6) No significant impact of surfactant on electroextraction was seen using qualitative tests. However, the interface length changed upon the addition of surfactant. Therefore, the study of the effect of surfactant on electroextraction calls for a device design giving constant interface length with and without surfactant. Also, quantitative analysis of the effect of surfactant on electroextraction needs to be done.

Future work of this research lies in the integration of electroextraction with lab-on-chip device as mentioned in section 2.2. Also, the effect of different analytes and solvents on electroextraction has to be studied.

Appendix

MATLAB code for extracting a and b values from images

```
clc
i=imshow('E:\4.png')
h=imfreehand(gca)
roi=createMask(h);
[row,col]=find(roi);
i1=imread('E:\4.png');
RGBpixels=impixel(i1,col,row);
labImg = rgb2lab(RGBpixels);
aChannel = labImg(:,2);
bChannel = labImg(:,3);
nr1=size(aChannel,1);
nr2=size(bChannel,1);
sum1=0;
sum2=0;
for i = 1:nr1
p=aChannel(i,1);
sum1=sum1+p;
end
avg_avalue=sum1/nr1
for j = 1:nr2
p=bChannel(j,1);
sum2=sum2+p;
end
avg_bvalue=sum2/nr2
min_a = min(min(aChannel));
max_a = max(max(aChannel));
min_b = min(min(bChannel));
max_b = max(max(bChannel));
```

References

[1] C. Shi, Y. Jing, J. Xiao, X. Wang, and Y. Jia, “Liquid-liquid extraction of lithium using novel phosphonium ionic liquid as an extractant,” Hydrometallurgy, vol. 169, pp. 314–320, May 2017.
[2] J. Comer and K. Tam, “Lipophilicity Profiles: Theory and Measurement,” in Pharmacokinetic Optimization in Drug Research, John Wiley & Sons, Ltd, 2007, pp. 275–304.
[3] “Applications Of Ionic Liquids In The Removal Contaminants From Flow Chart Liquidtion Flowchart Samples,” Arrowscan. [Online]. Available: https://www.arrowscan.com/flow-chart-of-liquid-liquid-extraction/applications-of-ionic-liquids-in-the-removal-of-contaminants-from/.
[4] U. Novak, A. Pohar, I. Plazl, and P. Žnidaršič-Plazl, “Ionic liquid-based aqueous two-phase extraction within a microchannel system,” Sep. Purif. Technol., vol. 97, pp. 172–178, Sep. 2012.
[5] P. Mary, V. Studer, and P. Tabeling, “Microfluidic Droplet-Based Liquid−Liquid Extraction,” Anal. Chem., vol. 80, no. 8, pp. 2680–2687, Apr. 2008.
[6] P. A. L. Wijethunga, Y. S. Nanayakkara, P. Kunchala, D. W. Armstrong, and H. Moon, “On-chip drop-to-drop liquid microextraction coupled with real-time concentration monitoring technique,” Anal. Chem., vol. 83, no. 5, pp. 1658–1664, 2011.
[7] S. Paul and H. Moon, “Separation of binary solution by liquid-liquid microextraction on EWOD digital microfluidics,” 2017 IEEE 12th Int. Conf. Nano/Micro Eng. Mol. Syst. NEMS 2017, pp. 342–345, 2017.
[8] I. Benjamin, “Mechanism and Dynamics of Ion Transfer Across a Liquid-Liquid Interface Author (s): Ilan Benjamin Published by : American Association for the Advancement of Science Stable URL : http://www.jstor.org/stable/2881972,” vol. 261, no. 5128, pp. 1558–1560, 2008.
[9] N. J. Petersen, H. Jensen, S. H. Hansen, K. E. Rasmussen, and S. Pedersen-Bjergaard, “Drop-to-drop microextraction across a supported liquid membrane by an electrical field under stagnant conditions,” J. Chromatogr. A, vol. 1216, no. 9, pp. 1496–1502, 2009.
[10] T. Hahn and S. Hardt, “Concentration and size separation of DNA samples at liquid-liquid interfaces,” Anal. Chem., vol. 83, no. 14, pp. 5476–5479, 2011.
[11] C. D. M. Campos, J. K. Park, P. Neužil, J. A. F. Da Silva, and A. Manz, “Membrane-free electroextraction using an aqueous two-phase system,” RSC Adv., vol. 4, no. 90, pp. 49485–49490, 2014.
[12] https://media.scbt.com/product/11/51/z/115188.jpg
[13] M. Lichtarowicz, “Colorants,” The Essential Chemical Industry online. [Online]. Available: http://www.essentialchemicalindustry.org/materials-and-applications/colorants.html.
[14] R. J. Soukup-Hein, M. M. Warnke, and D. W. Armstrong, “Ionic Liquids in Analytical Chemistry,” Annu. Rev. Anal. Chem., vol. 2, no. 1, pp. 145–168, 2009.
[15] G. W. Meindersma, A. (J. G. . Podt, M. G. Meseguer, and A. B. de Haan, “Ionic Liquids as Alternatives to Organic Solvents in Liquid-Liquid Extraction of Aromatics,” in Ionic Liquids IIIB: Fundamentals, Progress, Challenges, and Opportunities, pp. 57–71.
[16] J. Lee, H. K. Lee, K. E. Rasmussen, and S. Pedersen-Bjergaard, “Environmental and bioanalytical applications of hollow fiber membrane liquid-phase microextraction: A review,” Anal. Chim. Acta, vol. 624, no. 2, pp. 253-268[1] J. Lee, H. K. Lee, K. E. Rasmussen, and, Aug. 2008.
[17] D. Needham, K. Kinoshita, and A. Utoft, “Micro-surface and -interfacial tensions measured using the micropipette technique: Applications in ultrasound-microbubbles, oil-recovery, lung- surfactants, nanoprecipitation, and microfluidics,” Micromachines, vol. 10,

no. 2, 2019.
[18] N. Thi Hai van, N. Tat Thang, J. Di, and M. Guo, “Predicting color change in wood during heat treatment using an artificial neural network model,” Bioresources, vol. 13, pp. 6250–6264, 2018.
[19] “1-Octanol,” National Center for Biotechnology Information. PubChem Compound Database. [Online]. Available: https://pubchem.ncbi.nlm.nih.gov/compound/1-octanol#section=2D-Structure.

Biographical Information

Subhadeep Chakraborti received his bachelor degree from Dr. A.P.J. Abdul Kalam Technical University, India in 2015. He joined The University Of Texas At Arlington in 2017. There, he was a member of Integrated Micro/Nanofluidics Lab. His research interest includes digital microfluidics and extraction sciences.